17th World Conference on Earthquake Engineering, 17WCEE
Sendai, Japan - September 13th to 18th 2020

Scaling Relationship of Source Parameters for Crustal Earthquakes Assuming Constant Stress Drop

K. Hikima [1], A. Shimmura [2]

[1] *Specialist, TEPCO Research Institute, Tokyo Electric Power Company Holdings, Inc., hikima.kazuhito@tepco.co.jp*
[2] *Nuclear Asset Management Department, Tokyo Electric Power Company Holdings, Inc., shimmura.akihiro@tepco.co.jp*

Abstract

The scaling relationships among source parameters (e.g., seismic moment M_0, rupture area S, and fault length L) are important for source physics studies and seismic hazard analysis. Although the relationships have been classically studied by assuming self-similarity, the self-similar models do not hold for large crustal earthquakes due to the width limitation of the seismogenic layer. Various scaling relations for crustal earthquakes have been proposed by many authors, but most models result in a static stress drop that depends on the earthquake size. In contrast, for example, Anderson *et al.* (2017) for the M–L relation and Hikima and Shimmura (2020) (hereafter referred to as H&S) for M_0–S proposed scaling relationships that satisfy the constant stress drop for a wide magnitude range. They formulated scaling relations based on the theoretical static stress drop formula for a rectangular fault model. Although H&S showed good agreement with the existing data from medium to large earthquakes, that study did not discuss small to medium events in detail.

In this study, to advance the work in H&S, we discuss a scaling relation that assumes a constant stress drop for a wide seismic moment range, and show that the scale-independent stress drop basically holds for a wide range of earthquake magnitudes. For example, the figure shows the stress drop values calculated with the formulas of Chinnery (1964, 1969) for the event data used in H&S. Although the scatter of stress drop for small events is relatively large, no obvious dependence on the earthquake size is seen. The average value is about 3 MPa, which is almost same as that of H&S.

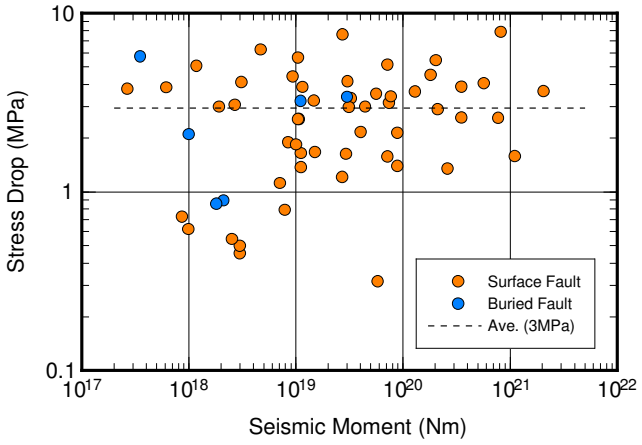

Fig. Relationship between seismic moment and static stress drop estimated assuming rectangular fault model

Keywords: Crustal earthquake; Scaling relationship; Static stress drop; Long length fault

1. Introduction

The scaling relationship among source parameters (e.g., seismic moment M_0, rupture area S, and fault length L) is important for earthquake source physics and seismic hazard analysis. Therefore, such relationships have been studied for a long time. The famous study by Kanamori and Anderson [1] revealed that the seismic moment and rupture area have the scaling relation of $M_0 \approx S^{3/2}$. The result means that a self-similar relation exists among length L, width W, and slip D, and also that the static stress drop $\Delta\sigma$ is constant from small to large earthquakes. The rupture widths of large earthquakes were not saturated in Kanamori and Anderson [1] because most of them were oceanic inter-plate earthquakes. However, for crustal earthquakes, an upper limit of the fault width exists due to the limit width of the crustal seismogenic layer. In these cases, the self-similarity does not hold. Therefore, for crustal earthquakes, scaling relations different from those of inter-plate earthquakes have been proposed.

For large crustal earthquakes, Scholz [2] proposed the so-called L-model, in which the slip is proportional to the rupture length but not to the width. Hanks and Bakun [3] suggested a bilinear scaling, in which a self-similar relation holds for small earthquakes and the L-model is adopted for large earthquakes. In contrast, Romanowicz [4] and Romanowicz and Ruff [5] advocated that the W-model, in which the slip is proportional to the rupture width, is appropriate for large earthquakes. Although those scaling relations are also bilinear, the slope of the equations for large earthquakes is different from that of the L-model because the assumed physical conditions are different. Although the static stress drop becomes constant in the scaling relation based on the W-model, the value varies depending on fault length in the scaling based on the L-model. Murotani *et al.* [6] quantified the idea of Irikura and Miyake [7] and proposed a scaling relation that is also applicable for small to long faults. In the relation, the power of the M_0–S scaling relation changes to $M_0 \approx S^{3/2}$, S^2, and S^1 as the size of earthquakes varies from small to large. The static stress drop, however, changes at each stage, because the model combines three different physical conditions into one scaling relation.

As mentioned above, whether the static stress drop for crustal earthquake is constant or varies with size is still debated, and the attitude toward them affects the shape of scaling relations. Here, we think that the static stress drop is nearly constant regardless of the earthquake size, if the stress drop is considered as a physical property of the crust. Based on this position, Hikima and Shimmura [8] (hereafter H&S) formulated a M_0–S scaling relation that realizes a scale-independent stress drop condition by referring to the analytical solution for rectangular faults (Chinnery [9], [10]) in a fashion similar to that of Anderson *et al.* [11]. H&S introduced a correction factor to compensate for the difference in physical models between Chinnery's model and ordinary crack models to compare them with the existing earthquake parameters. The proposed formula agreed well with data for medium to large magnitude earthquakes, and it means the constant stress drop holds for relatively large earthquakes. However, for small earthquakes whose width does not saturate the seismogenic width, discussions using the event data were not sufficient.

In this paper, we first outline the results of H&S [8] because this study contains the basic idea of our studies. Then, we discuss the method for calculating the static stress drop and scaling relations for relatively small earthquakes. After that, we apply them to the event data and verify whether the stress drops for a wide magnitude range are almost constant. Note that, because distinct discrepancies among fault types were not recognized in our previous study, we discuss fault types without classification in this paper, unless otherwise specified.

2. M_0–S scaling relation assuming rectangular fault

2.1 Formulation for surface faults

H&S discussed the M_0–S scaling relation mainly based on the formula of the static stress drop for a rectangular vertical strike-slip surface fault [9] in an approach similar to that of Anderson *et al.* [11], who

discussed the *M–L* scaling relations using this formula. Here we summarize these approaches and show the proposed scaling relations.

According to Chinnery [9] and Anderson *et al*. [11], the static stress drop at the surface center of a rectangular vertical strike-slip surface fault with a uniform slip distribution is expressed by Eq. (1) using the parameters in Fig. 1.

$$\Delta\sigma = \frac{\mu}{2\pi}\frac{D}{W}C(\gamma),\ C(\gamma) = 2\cos\gamma + 3\tan\gamma - \frac{\cos\gamma\sin\gamma(3+4\sin\gamma)}{(1+\sin\gamma)^2}, \tag{1}$$

where we used the relation $\tan\gamma = W/L_h$ according to Anderson *et al.* [11].

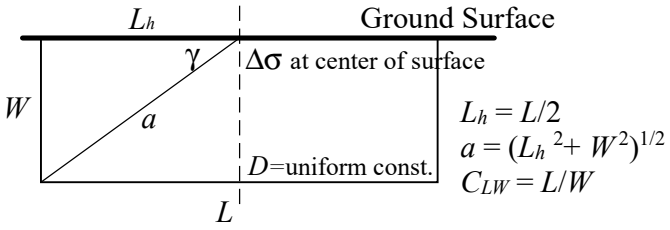

Fig. 1 – Schematic of rectangular surface fault.

To calculate the relation between the static stress drop and the seismic moment, we solve D from Eq. (1) and perform the substitution $M_0 = \mu DS$ to obtain

$$M_0 = \frac{2\pi}{C(\gamma)}\Delta\sigma SW\ . \tag{2}$$

The coefficient $C(\gamma)$ depends on the aspect ratio C_{LW}, which means that M_0 is evaluated through the fault shape and the static stress drop. Eq. (2) is applicable for any size fault, from small to large events.

However, because the boundary condition of Chinnery's formula is different from ordinary crack models, there are some drawbacks. One is that the calculated stress drop becomes infinite at the crack tip, and the second is that the evaluated stress drop is exact only at the center of the surface side for a surface fault, or at the center of the plane for a buried fault. Although there are such problems, it has the advantage of providing a simple analytical solution, which is useful for formulation of a scaling relation. To overcome these drawbacks, we also introduced a correction factor, which considers that approximately twice the Chinnery value corresponds to the value obtained by the crack model. A detailed explanation for this factor and its verification is provided in H&S [8]. When the correction factor is applied to Eq. (2), the relation that can be comparable with that in the ordinary crack model becomes

$$M_0 = \frac{\pi}{C(\gamma)}\Delta\sigma SW\ . \tag{3}$$

When Eq. (3) is applied to crustal earthquakes, the aspect ratio C_{LW} is constant until its width reaches the saturated rupture width W_{max}, and the rupture area becomes $S = LW = C_{LW}W^2$. However, when the rupture width is saturated, the width becomes the fixed value $W = W_{max}$ and C_{LW} is no longer constant. Therefore, Eq. (3) can be rewritten as follows:

$$M_0 = \frac{\pi}{\sqrt{C_{LW}}C(\gamma)}\Delta\sigma S^{3/2}\ , \qquad \text{for } L/C_{LW} < W_{max}, \tag{4a}$$

$$M_0 = \frac{\pi}{C(\gamma)}\Delta\sigma W_{max}S\ , \qquad \text{for } L/C_{LW} \geqq W_{max}. \tag{4b}$$

Furthermore, we can take the logarithm of both sides and rearrange these equations as relations between log M_0 and log S:

$$\log M_0 = \frac{3}{2}\log S + \log \Delta\sigma + \log\left\{\frac{\pi}{\sqrt{C_{LW}}C(\gamma)}\right\}, \qquad \text{for } L/C_{LW} < W_{max}, \tag{5a}$$

$$\log M_0 = \log S + \log \Delta\sigma + \log\left\{\frac{\pi}{C(\gamma)}W_{max}\right\}, \qquad \text{for } L/C_{LW} \geqq W_{max}. \tag{5b}$$

These relations maintain the constant stress drop condition for small to large earthquakes. Regarding the form of the relations, the slope for the small to medium faults is 2/3, while the slope for long large faults asymptotically tends to 1 on a logarithmic graph. These are consistent with the self-similar model and the W-model, respectively, and are comparable with the first and third stages of the three-stage scaling model [6]. The slope for moderate faults, which corresponds to the second stage of the three-stage model, changes according to $C(\gamma)$, which depends on the aspect ratio of the fault.

2.2 Comparison with event data

To indicate the validity of the formulas, H&S compared the proposed formulas with existing event data and determined an approximately proper stress drop. The data were taken from published papers [6], [12], [13], [14] and listed in H&S [8]. The comparison with the data is depicted in Fig. 2, in which the proposed formula is plotted by a solid curve calculated with W_{max} =18 km and $\Delta\sigma$ = 3 MPa. The scaling relation assuming a constant stress drop shows good agreement with the data in a similar degree with the three-stage scaling relationship [6]. Therefore, it can be said that a scale-invariant stress drop is almost appropriate for crustal earthquakes.

However, the value of the stress drop and the saturated rupture width were determined only for relatively large earthquakes, which are depicted as filled symbols in Fig. 2. For small earthquakes, which mainly do not saturate the seismogenic layer, evaluation has been insufficient, and it is not clear whether the stress drop is constant or almost the same as that for large events. Therefore, we will again consider the stress drop for small earthquakes in the following sections.

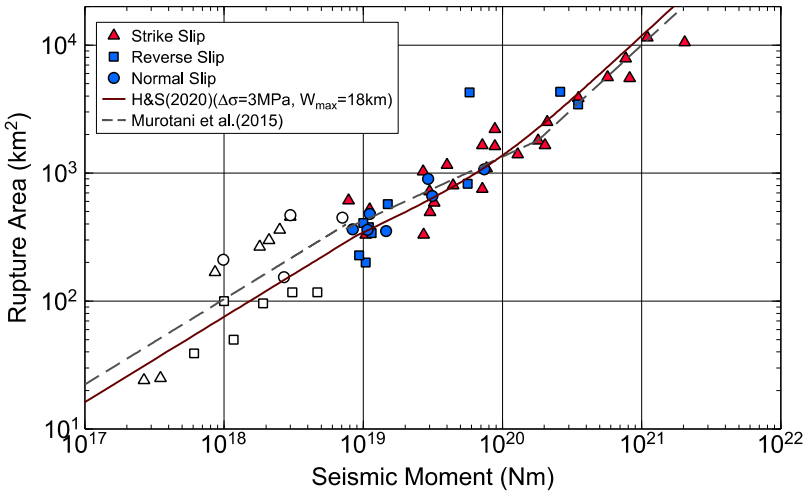

Fig. 2 – Scaling relations discussed in H&S (solid curve). The three-stage scaling relation by Murotani *et al.* [6] (dashed curve) is also plotted. The filled and open symbols represent the data that were used and not used, respectively, to determine the proper stress drop.

3. Stress drop of small events

In the previous paper [8], we applied the rectangular fault model to estimate the stress drop for small events in a way similar to that for the surface fault model, but the reference model was a buried fault [10]. The formula for scaling between M_0 and S is as follows:

$$M_0 = \frac{3\pi}{4C'(\xi)} \Delta\sigma \xi^{1/2} S^{3/2}, \tag{6}$$

where $\xi = W/L = 1/C_{LW}$ and $C'(\xi) = (3 + 4\xi^2)/\sqrt{1 + \xi^2}$.

This formulation is consistent with the concept for larger faults, in the sense that all events are based on the rectangular fault model. However, because the error in the introduced correction factor is relatively large for faults having a small aspect ratio [8], it may be more appropriate to use another physical model, such as the circular crack model [15], to calculate the static stress drop.

When a circular crack that has same area as a rectangular fault (such a model is sometimes called an "equivalent circular crack") is used to calculate the stress drop, the scaling relation is written as

$$M_0 = \frac{16}{7} \Delta\sigma \left(\frac{S}{\pi}\right)^{3/2}, \tag{7}$$

where $S = LW$. Consequently, from Eqs. (6) and (7), if the stress drops for rectangular and circular faults are denoted as $\Delta\sigma_s$ and $\Delta\sigma_c$, respectively, and the aspect ratio for a rectangular fault is assumed as $\xi = 1$, the relation between $\Delta\sigma_s$ and $\Delta\sigma_c$ for faults having the same M_0 becomes $\Delta\sigma_c = 1.16\Delta\sigma_s$. Conversely, if the stress drops are identical, the M_0 calculated for a square fault becomes 16 % larger than the value for a circular fault.

These relations, whose stress drop values are set as 3 MPa, are plotted in Fig. 3 with the data used in Fig. 2. The curve assuming the buried rectangular fault model mostly overlaps the curve for a surface fault; therefore, these relations cannot be distinguished clearly. In contrast, the curve assuming a circular crack shows an M_0 smaller than that for a square fault having an equal fault area and, as a result, it seems to match better with small event data than it does with other relations. Therefore, if the circular crack model is assumed for small events and it is combined with formulas for a surface fault model for large events, those scaling relations can fit the data better when the stress drop is constant. However, a gap exists at the boundary between the two curves because the assumed fault models are different. Clearly, it is not realistic for the fault shape to change suddenly from circular to rectangular, even if it reaches the ground surface or is cut off from the whole seismogenic layer. Therefore, it is expected that the scaling relations vary gradually between small and large fault stages. Nevertheless, it seems to be difficult to determine those relations only from the existing event data, in part due to the estimated error of source parameters. Despite the persistent difficulty in determining complete scaling relations, it was shown that a constant stress drop model is basically consistent with event data over a wide seismic moment range.

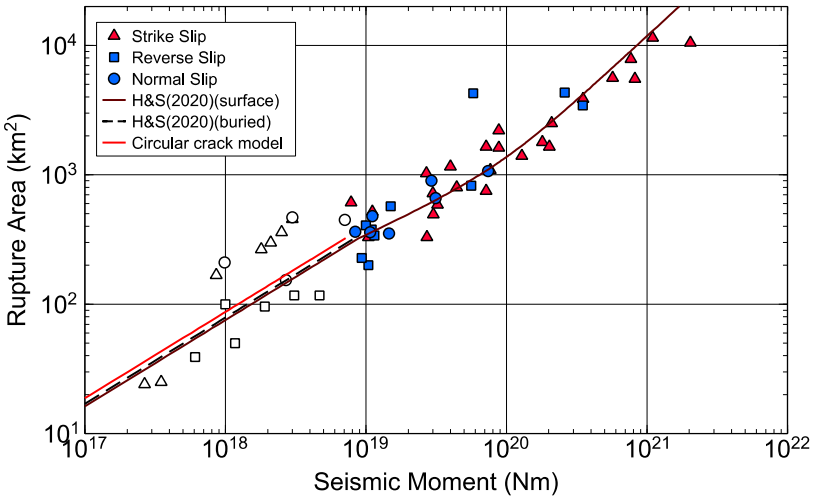

Fig. 3 – Scaling relation for small events. The three scaling curves are based on surface and buried rectangular faults and a circular fault. Event data used in Fig. 2 are also plotted.

4. Stress drop considering fault shape

We calculated static stress drops considering the shape of each fault and checked the values directly. The stress drop values were calculated using Eqs. (3) and (6), which were derived by Chinnery [9], [10] and applied the correction factor adopted by H&S [8]. The target event data are same as those used in H&S. To determine which equations to apply, each event was classified as a surface fault or a buried fault by comprehensively considering the top depth of the fault and previous studies.

The stress drop values calculated with a rectangular fault model are plotted in Fig. 4(a). Different symbols are used to distinguish between surface faults and buried faults, and the number of buried faults was six. However, this classification of faults is tentative, and we may change it in the future. However, we think that the influence of any particular fault classification on the discussion in this study is unlikely to be critical, because the difference between those formulas is not large, as shown in Fig. 3. The average stress drop is 2.9 MPa and the value is consistent with that given in H&S. Furthermore, it is notable that the value is independent of earthquake size, though the variance is not small.

Moreover, we also calculated the stress drop values assuming an equivalent circular crack in an approach similar to that of an existing study [16] using Eq. (7). These are plotted in Fig. 4(b). The average value is 4.1 MPa and it is larger than those of Fig. 4(a). Although these relations generally do not contradict the discussion in the previous section, the degree of overestimation by the circular crack model is greater than expected. Additionally, the variance is larger than that in Fig. 4(a). From these discrepancies, it seems that the stress drop calculated by the circular fault model tends to be overestimated and unstable. In addition, the application of and equivalent circular crack for a long crustal earthquake has already been discussed in a previous study and its use is not recommended for long events [16]. Therefore, the equivalent circular crack should be considered as not suitable for medium to large events.

For small earthquakes, although their number is few, the average values assuming rectangular and circular fault models were 2.7 and 3.1 MPa, respectively. The differences between these models are trivial and both values are comparable with those of medium to large events; therefore, the circular crack model also seems to be applicable to small earthquakes, as described before.

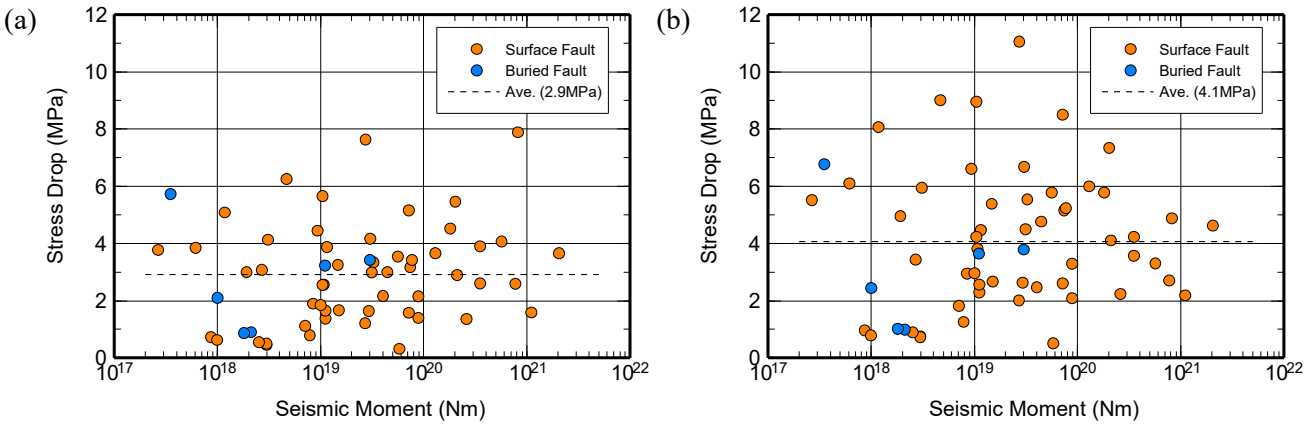

Fig. 4 – Stress drop for the event data used in Fig. 2. (a) Stress drop calculated with a rectangular fault model. (b) Stress drop calculated with an equivalent circular crack model.

Next, to discuss small events in more detail, we also used another database. Those data are based mainly on Thingbaijam *et al.* [17], who processed the SRCMOD database [18]. We used them complementarily in the Appendix of H&S. The stress drop calculated with the rectangular fault model is shown in Fig. 5. Overall, the calculated values are somewhat lower than those in Fig. 4(a). Although this trend is already shown in H&S, its cause is still under consideration. However, here we focused on the difference between surface and buried faults and the size dependency.

The differences in the average stress drop between buried and surface faults are not clear, but the degree of variance appears to be distinctly different, which means that the variance of stress drop for buried faults (mainly small events) is greater than that for surface faults (mostly large events). Another feature of the plot is that no obvious size dependence is seen in these data, as in Fig. 4(a). Therefore, a scale-independent stress drop is seen in this database.

In this study, we examined two datasets, and consequently no clear scale dependence of the static stress drop was observed in either database. Conversely, the stress drop variance for small and/or buried faults seems to be greater than that for large events. The cause of the difference in these variances should be considered in detail in the future. However, we think one reason is that the fault size for small events is not very limited and depends on local stress conditions, while large events are restricted by the thickness of the seismogenic layer and affected by regional stress conditions.

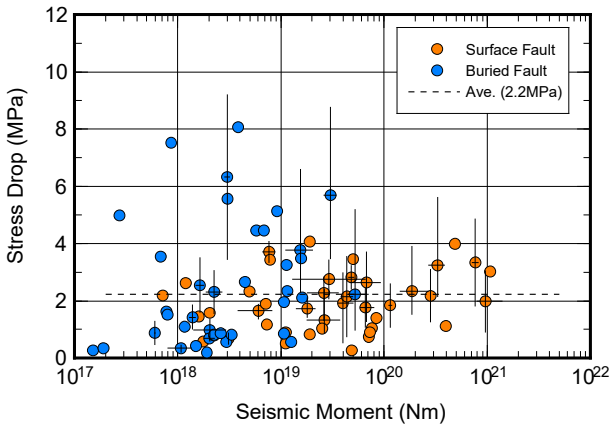

Fig. 5 – Stress drop for the event data taken from Thingbaijam *et al*. [17]. These values were calculated with the rectangular fault formulas. When multiple rupture models exist for the same event, the average values are plotted, and the bars indicate the corresponding ranges.

5. Discussion

As we have seen, the scaling relation with a constant stress drop agrees well with the past event data, and no obvious size dependence could be recognized by directly calculating the stress drops. However, we also know that many researchers have concluded that the stress drop depends on scale. Their conclusions are based on various reasons, for example, observed waveform data, analyzed source parameters, and dynamic rupture simulations. As an example of recent research, Thingbaijam *et al.* [17] suggested a scale-dependent stress drop by examining the ratio D/W as a proxy for average stress drop. The ratio D/W, which corresponds to strain, is related to the stress drop by the following equation:

$$\Delta\sigma = C\mu\frac{D}{L_c}, \tag{8}$$

where L_C is the characteristic length of the event (here, the width W) and C is a constant that depends on the fault shape (e.g., Lay and Wallace [19]). Eq. (1) in this paper is similar, but C in Eq. (1) is a variable depending on the fault shape.

We depict the D/W ratio for the event data used by H&S in Fig. 6(a). The ratio indeed tends to increase as the earthquake size becomes larger, and therefore the stress drop seems to become more dependent on event size. As seen in Eq. (8), that is because the slip D increases despite the width W becoming nearly constant for larger crustal earthquakes. In addition, the assumption of a constant C also contributes to the estimation of the scale-dependent stress drop. However, if the rectangular fault model is used, C is no longer constant, but it becomes a variable depending on its aspect ratio, as exhibited in Eq. (1). To illustrate the relationship by example, the fault displacements for some models were calculated using the

rectangular fault model formula and are listed in Table 1. As shown in the table, even after the fault width is saturated at W_{max} = 18 km, the slip D becomes larger and the D/W ratio also becomes greater. These relations are also plotted in Fig. 6(a) as a red curve. The expected ratios are mostly consistent with the trend of the D/W distribution of fault parameters. This suggests that the constant stress drop condition is generally maintained if the fault shape is properly considered.

Table 1 – Fault parameters obtained using the scaling relation by H&S

L (km)	6	10	15	18	20	30	40	50	80	100	200	300	500	1000
W (km)	6	10	15	18	18	18	18	18	18	18	18	18	18	18
M_0 (Nm)	3.30e17	1.53e18	5.16e18	8.92e18	1.09e19	2.33e19	3.85e19	5.50e19	1.06e20	1.40e20	2.99e20	4.54e20	7.61e20	1.53e21
D (m)	0.28	0.46	0.70	0.83	0.92	1.31	1.62	1.85	2.23	2.35	2.52	2.55	2.56	2.57
D/W in m	4.64e-05	4.64e-05	4.64e-05	4.64e-05	5.11e-05	7.28e-05	9.00e-05	1.03e-04	1.24e-04	1.31e-04	1.40e-04	1.42e-04	1.42e-04	1.43e-04

* Assumed as $\Delta\sigma$ = 3 MPa and D was estimated assuming $\mu = 3.3\text{x}10^{10}$ N/m^2

For reference, the same relations for the modified data of Thingbaijam *et al.* [17] also are depicted in Fig. 6(b). The scale dependency is seen also in these data, although it is less clear. The D/W ratio is slightly lower overall than in the former data, but it is consistent with the tendency found in Fig. 5, which means that the lower ratio reflects the average stress drop being lower than 3 MPa. Therefore, if we adopt lower stress drop values in the calculation of the theoretical ratio, the scaling relation with a rectangular fault model will become consistent, and these data show a constant stress drop condition.

As thus far described, the scaling relationship for a crustal earthquake with constant stress drop can be configured if its fault shape is taken into account properly. In addition, the scale independence was shown also by the stress drop values directly calculated by the rectangular model. However, in practice, not a little difficulty will be encountered in determining the proper coefficients from existing source parameters, due to considerable variation of those parameters. Such studies need to be carried on continuously to advance hazard analyses in the future.

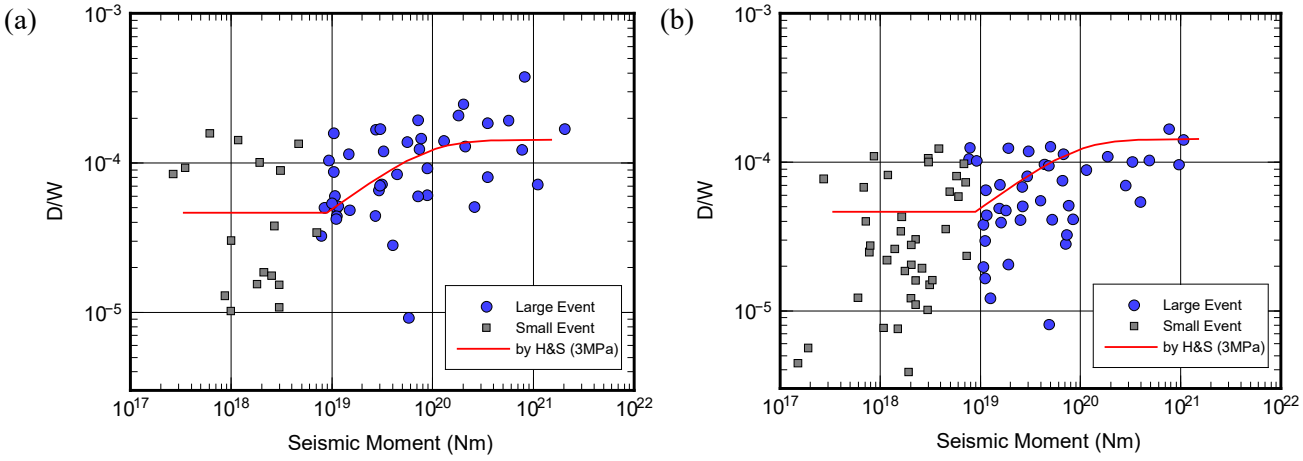

Fig. 6 – D/W ratio for the event data. (a) Plots of the data used in H&S. (b) Plots of the data in Thingbaijam *et al.*[17] The ratios calculated using the formula proposed in H&S (assumed $\Delta\sigma$ = 3 MPa and W_{max} = 18 km) are drawn as red curves.

6. Conclusion

In this short paper, we have explained the scaling relationship for crustal earthquakes by assuming a constant stress drop, in line with Hikima and Shimmura [8]. Based on this relation, we have advanced the discussion for applying this scaling relation to small earthquakes. Then, stress drop values for a wide size range were

calculated using rectangular fault models, and the scale dependence of the stress drop was examined directly. The findings and our comments on these evaluations are as follows:

The constant (scale-independent) stress drop holds over a wide size range, even for crustal earthquakes.

In contrast, the variance for small earthquakes tends to be larger than that for medium to large events.

Transitions in the scaling relationship occur gradually rather than suddenly. Such transitions mark the change from small events to saturated events, as well as a change in the slope for the scaling relation after the fault saturates seismogenic layer.

To represent those changes, it is very important to consider the fault shape explicitly.

It is not easy to uniquely determine the scaling relation from existing source parameters, in practice. However, considering that a prediction formula based on physical models can lead to improvements in the reliability of hazard analyses, it is important to consider the scaling relationship also with the condition that the average static stress drop is constant.

7. Acknowledgements

The authors would like to express appreciation to the previous researchers who compiled and provided source parameters of past earthquakes in their papers. Most figures were made using the Generic Mapping Tools (Wessel and Smith [20]).

8. References

[1] Kanamori H, Anderson DL (1975): Theoretical basis of some empirical relations in seismology. *Bull. Seismol. Soc. Am.*, **65**, 1073–1095.

[2] Scholz C (1982): Scaling laws for large earthquakes: Consequences for physical models. *Bull. Seismol. Soc. Am.*, **72**, 1–14.

[3] Hanks TC, Bakun WH (2002): A bilinear source-scaling model for M–log A observations of continental earthquakes. *Bull. Seismol. Soc. Am.*, **92**, 1841–1846.

[4] Romanowicz B (1992): Strike-slip earthquakes on quasi-vertical transcurrent faults: Inferences for general scaling relations. *Geophys. Res. Lett.*, **19**, 481–484.

[5] Romanowicz B, Ruff LJ (2002): On moment-length scaling of large strike slip earthquakes and the strength of faults. *Geophys. Res. Lett.*, **29**, 12, 1604.

[6] Murotani S, Matsushima S, Azuma T, Irikura K, Kitagawa S (2015): Scaling relations of source parameters of earthquake occurring on inland crustal mega-fault systems. *Pure Appl. Geophys.*, **172**, 1371–1381.

[7] Irikura K, Miyake H (2011): Recipe for predicting strong ground motion from crustal earthquake scenarios. *Pure Appl. Geophys.*, **168**, 85–104.

[8] Hikima K, Shimmura A (2020): Moment–Area Scaling Relationship Assuming Constant Stress Drop for Crustal Earthquakes. *Bull. Seismol. Soc. Am.*, **110**, doi: 10.1785/0120180339.

[9] Chinnery, MA (1964): The strength of the Earth's crust under horizontal shear stress. *J. Geophys. Res.*, **59**, 2085–2089.

[10] Chinnery, MA (1969): Theoretical fault models. *Pub. Dominion Obs*, **17**, Ottawa, 211-223.

[11] Anderson JG, Biasi GP, Wesnousky SG (2017): Fault-scaling relationships depend on the average fault-slip rate. *Bull. Seismol. Soc. Am.*, **107**, 2561–2577.

[12] Somerville PG, Irikura K, Graves R, Sawada S, Wald D, Abrahamson N, Iwasaki Y, Kagawa T, Smith N, Kowada A (1999): Characterizing crustal earthquake slip models for the prediction of strong ground motion. *Seismol. Res. Lett.*, **70**, 59–80.

[13] Stirling M, Rhoades D, Berryman K (2002): Comparison of earthquake scaling relations derived from data of the instrumental and preinstrumental era. *Bull. Seismol. Soc. Am.*, **92**, 812–830.

[14] Hashimoto T (2007): The surface length of earthquake fault and the moment magnitude. *Abstracts for Japan Geoscience Union meeting*, S145-013.

[15] Eshelby, JD (1957): The determination of the elastic field of an ellipsoidal inclusion, and related problems. *Proc. Math. Phys. Sci.*, **241**, 376–396.

[16] The Headquarters for Earthquake Research Promotion (2017): Strong ground motion prediction method for earthquakes with specified source faults (“Recipe”). https://www.jishin.go.jp/main/chousa/17_yosokuchizu/recipe.pdf

[17] Thingbaijam, KKS, Mai PM, Goda K (2017): New empirical earthquake source-scaling laws. *Bull. Seismol. Soc. Am.*, **107**, 225–2246.

[18] Mai PM, Thingbaijam KKS (2014): SRCMOD: An online database of finite-fault rupture models. *Seismol. Res. Lett.*, **85**, 1348–1357.

[19] Lay T, Wallace TC (1995): Modern global seismology., Academic press, Inc., California, 521 pages.

[20] Wessel P, Smith WHF (1998): New, improved version of Generic Mapping Tools released. *EOS Trans. Am. Geophys. Union* **79**, 579.

